MODELING THE GROUND LEVEL ENHANCEMENT GLE 77 EVENT OF NOVEMBER 11, 2025, AND ITS EFFECTS ON THE EARTH'S ENVIRONMENT

Peter I. Y. I. Velinov, Krasimir Krastev, Radostin Pavlov

Space Research and Technology Institute – Bulgarian Academy of Sciences
e-mail: PeterIYVelinov@gmail.com

Keywords: *Ground Level Enhancement (GLE 77), Galactic Cosmic Rays, Ionization*

Abstract: *GLE 77 of November 11, 2025, which is the largest GLE in the last 20 years, was quantitatively studied. Ionization profiles were obtained in the interval from 0 to 100 km in the Earth's atmosphere.*

МОДЕЛИРАНЕ НА СЪБИТИЕТО GLE 77 ОТ 11 НОЕМВРИ 2025 Г. И НЕГОВИТЕ ЕФЕКТИ ВЪРХУ ОКОЛОЗЕМНОТО КОСМИЧЕСКО ПРОСТРАНСТВО

Петър Велинов, Красимир Кръстев, Радостин Павлов

Институт за космически изследвания и технологии – Българска академия на науките
e-mail: PeterIYVelinov@gmail.com

Ключови думи: *Повишаване интензитета на космическите лъчи на земното ниво – ГЛЕ 77, Галактически Космически Лъчи, Йонизация*

Резюме: *Количествено е изследвано ГЛЕ 77 от 11 ноември 2025 г., което се явява най-голямото ГЛЕ за последните 20 години. Получени са профилите на йонизация в интервала от 0 до 100 km в земната атмосфера.*

Introduction

The Sun is a major source of space weather disturbances, producing energetic phenomena such as solar flares and coronal mass ejections (CMEs), which can accelerate charged particles to high energies. These particles, known as solar energetic particles (SEPs), propagate through interplanetary space and may reach the Earth, where their access to the atmosphere is influenced by the geomagnetic field. Once they enter the atmosphere, primary particles interact with atmospheric nuclei, producing extensive cascades of secondary particles and contributing to the ionization of the atmospheric medium.

Ground Level Enhancements (GLEs) are rare solar energetic particle events characterized by an increase in secondary particle fluxes detected by ground-based neutron monitors. These events provide valuable information about the acceleration and propagation of solar particles, as well as their interactions with the Earth's magnetosphere and atmosphere. The magnitude and geographical distribution of the atmospheric response depend on the energy spectrum and angular distribution of the incident particles, atmospheric density, and geomagnetic rigidity cutoff.

On 11 November 2025, a strong solar energetic particle event, designated GLE #77, was recorded by the worldwide neutron-monitor network. The event was associated with an X5.1-class solar flare and exhibited a complex, multi-component particle distribution. Observations indicated a substantial enhancement in neutron-monitor count rates and elevated radiation levels at high-latitude aviation altitudes. These characteristics make GLE #77 an important case for investigating the atmospheric response to an intense solar particle event. [1, 2]

Numerical simulations provide an effective means of investigating the development of atmospheric particle cascades and the energy deposition associated with energetic particle

precipitation. In particular, the GEANT4 Monte Carlo simulation toolkit enables the modeling of particle transport, electromagnetic and hadronic interactions, secondary particle production, and energy deposition in matter. When applied to an atmospheric model, GEANT4 can be used to investigate the production and transport of secondary particles and to estimate the altitude dependence of ionization under specified primary-particle and atmospheric conditions.

The geomagnetic rigidity cutoff is an important parameter governing the access of charged primary particles to the Earth's atmosphere. Particles with rigidities below the effective cutoff are generally excluded from direct access along the corresponding allowed trajectories, whereas particles with sufficiently high rigidities can penetrate the geomagnetic shielding. Consequently, variations in the rigidity cutoff can modify the primary particle population entering the atmosphere and, in turn, affect the altitude distribution and magnitude of atmospheric ionization. Comparing simulations for different geomagnetic cutoff conditions therefore provides a way to investigate the sensitivity of atmospheric ionization profiles to geomagnetic shielding.

The aim of this study is to investigate the atmospheric response to energetic cosmic-ray particles using GEANT4, with particular emphasis on the calculation and comparison of ionization profiles under different geomagnetic rigidity cutoff conditions. The study considers the transport and interactions of primary particles in the atmosphere and the production of secondary particles that contribute to atmospheric energy deposition and ionization. By examining the resulting altitude-dependent profiles for different cutoff conditions, this work seeks to characterize the influence of geomagnetic shielding on the atmospheric response to energetic particle precipitation and to provide a numerical framework that can support the interpretation of observations associated with GLE #77.

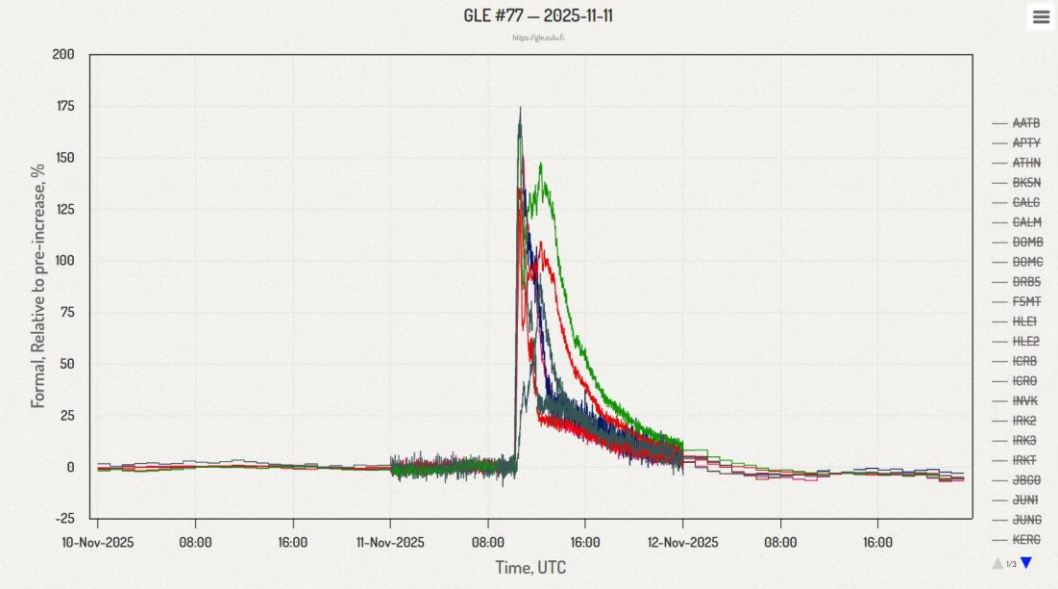


Fig. 1. The figure is taken from the worldwide neutron monitor database (https://gle.oulu.fi/#/)

Calculation methodology

The ion-pair production rate in the atmosphere was calculated by Monte Carlo simulation with the Geant4 toolkit (Agostinelli et al., 2003; Allison et al., 2016). The interactions of the primary particles and the development of the secondary cascades were modelled with the FTFP_BERT reference physics list, which combines the Fritiof string model at high energies with the Bertini intranuclear cascade at intermediate energies and is recommended for hadronic showers. The production threshold for secondary particles was set to 10 m, which is much shorter than the thickness of the scoring layers.

Atmospheric model. The geometry is centred on the centre of the Earth, which is a sphere of radius R_E = 6356.766 km. The atmosphere between 10 and 80 km altitude is represented by 35 concentric spherical shells, each 2 km thick. Each shell is filled with dry air (mass fractions N 0.755, O 0.232, Ar 0.013). Its density, temperature and pressure are taken from the U.S. Standard Atmosphere 1976 at the mid-altitude of the shell, after converting geometric altitude to geopotential altitude. The region between 80 and 100 km is treated as vacuum. All particles that reach altitudes below 10 km are stopped, because the ionization is not scored there.

Primary spectrum. The differential intensity of the galactic cosmic ray protons at the top of the atmosphere is described by the force-field approximation with the local interstellar spectrum of Castagnoli and Lal (1980):

(1) $J(T) = A \cdot T(T + 2m_p)(T + x + \varphi)^{(-\gamma)} / [(T + \varphi)(T + 2m_p + \varphi)]$, $x = a \cdot \exp(-bT)$,

where T is the kinetic energy in MeV, m_p is the proton rest energy, $\varphi = 530$ MV is the solar modulation potential, $A = 9.9 \times 10^8$, $a = 780$, $b = 2.4 \times 10^{-4}$ and $\gamma = 2.65$. Geomagnetic shielding is taken into account by a sharp vertical cutoff. The lower energy limit equals the kinetic energy that corresponds to the cutoff rigidity R_c:

(2) $T_c = [(R_c)^2 + m_p^2]^{(1/2)} - m_p$,

and the upper energy limit is 10 TeV.

Event generation and weighting. To sample the wide energy range efficiently, primary energies are drawn from a log-uniform distribution, $q(T) = 1/[T \cdot \ln(T_{max}/T_{min})]$. Each event receives the physical weight

(3) $w = \pi \cdot J(T) / q(T)$ [particles m^{-2} s^{-1}],

which is the flux through a unit area of the source sphere integrated over the inward hemisphere. All primaries start from one point on the sphere at 100 km altitude. Their directions follow the cosine law for an isotropic flux crossing a surface, with $\mu = \cos\theta = \xi^{(1/2)}$, where ξ is a uniform random number. The energy deposited in each step is assigned to the whole spherical shell in which the step occurred. Because the problem is spherically symmetric, this is equivalent to an isotropic source distributed uniformly over the whole sphere with scoring at a single location, and every simulated event contributes to all shells.

Ionization rate. The weighted mean energy deposit $\langle wE_i \rangle$ in shell i is converted to the ion-pair production rate as

(4) $q_i = \langle wE_i \rangle / [W \cdot (V_i/A_s)]$, $V_i/A_s = (r_1^3 - r_0^3)/(3R_s^2)$,

where $W = 34$ eV is the mean energy required to produce one ion pair in air, r_0 and r_1 are the inner and outer radii of the shell, and R_s is the radius of the source sphere. The statistical uncertainty of q_i is estimated as the standard error of the weighted mean,

(5) $\sigma_i = [(\langle (wE_i)^2 \rangle - \langle wE_i \rangle^2)/(N - 1)]^{(1/2)}$,

where N is the number of simulated events. Independent runs with different random seeds can be combined to reduce the uncertainty. The simulation runs in multithreaded mode, and the results of all threads are merged before normalization.

Atmospheric ionization by galactic cosmic rays via GEANT4

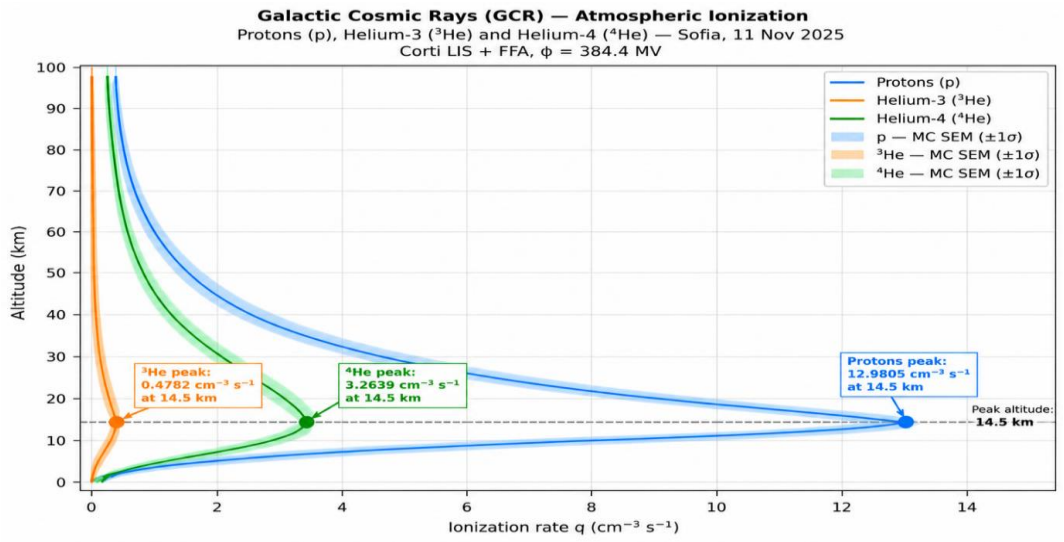


Fig. 2.

The atmospheric ionization induced by GLE 77 solar protons was computed with a Monte Carlo model based on the GEANT4 toolkit (version 11.4.2; Agostinelli et al., 2003; Allison et al., 2016) and the FTFP_BERT physics list. The atmosphere is represented by 100 concentric spherical shells of 1 km thickness between 0 and 100 km above a spherical Earth (R = 6371.2 km). The density, temperature and composition of each shell are taken from the NRLMSIS 2.1 empirical model for 11 November 2025, 10:30 UT, at the location of Sofia (42.70° N, 23.32° E) [ref. NRLMSIS 2.1]. The geomagnetic field inside the simulation domain is described by the IGRF-14 model for epoch 2025.86 [ref. IGRF-14].

For each primary energy, protons are injected at 100 km altitude with an isotropic (cosine-law) angular distribution over the downward hemisphere, and the full secondary cascade is followed. The energy deposited in each shell is converted into the number of ion pairs using a mean energy of W = 33.85 eV per ion pair in air, which gives the ionization yield function Y(E, h) per incident primary. The yield was calculated on a logarithmic grid of [17] kinetic energies between the cutoff energy and 30 GeV, with [N] simulated cascades per energy. The ion pair production rate is then obtained as

(6) $q(h) = \int_{E_c}^{E_{max}} \pi J(E) Y(E, h) dE,$

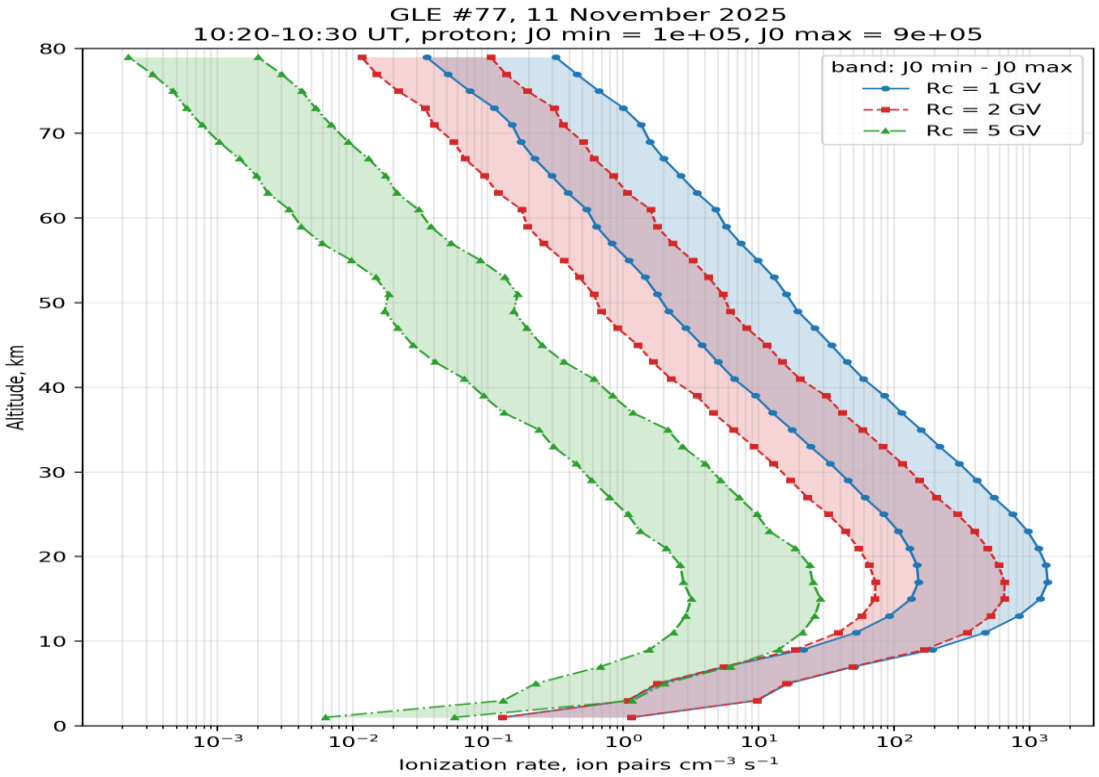
where J(E) is the differential intensity of solar protons above the atmosphere and E_c is the kinetic energy corresponding to the geomagnetic cutoff rigidity R_c. Assuming a sharp vertical cutoff, the yield function does not depend on R_c, so one set of simulations serves all cutoffs. Results are presented for R_c = 1, 2 and 5 GV, averaged over 2-km altitude bins from 0 to 80 km.

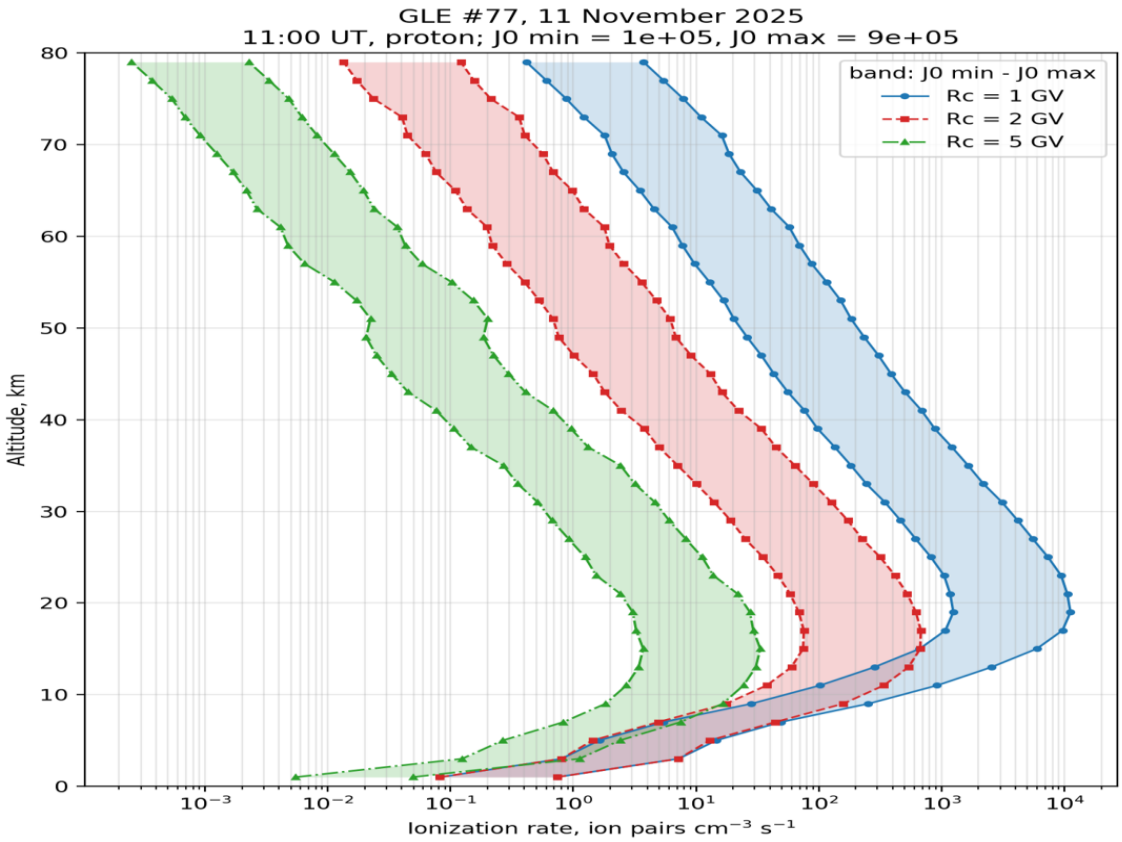
The spectral shapes of the solar protons were taken from the neutron-monitor analysis of Balabin et al. (2026): an exponential spectrum $J = J_0 \exp(-E/E_0)$ with E_0 = 0.73 GeV at 10:20–10:30 UT, a power law $J = J_0 E^{(-\gamma)}$ with γ = 4.2 at 11:00 UT, and exponential spectra with E_0 = 0.63 GeV at 11:30 UT and E_0 = 0.42 GeV at 15:00 UT. Because the normalization is uncertain, the calculations were performed for J_0 between 1×10^5 and 9×10^5 m^{-2} s^{-1} sr^{-1} GeV^{-1}, and the results are presented as the corresponding range of q.

The calculated profiles show a maximum at 15–19 km altitude. At 10:20–10:30 UT the maximum ionization rate is 1.5×10^2–1.4×10^3 cm^{-3} s^{-1} for R_c = 1 GV, 73–660 cm^{-3} s^{-1} for R_c = 2 GV and 3.2–29 cm^{-3} s^{-1} for R_c = 5 GV. The highest values are obtained at 11:00 UT for R_c = 1 GV (1.3×10^3–1.1×10^4 cm^{-3} s^{-1}), reflecting the large contribution of protons with rigidities between 1 and 2 GV in the power-law spectrum. As the spectrum softens, the ionization decreases, most strongly for high cutoffs: between 11:00 and 15:00 UT the maximum ionization rate for R_c = 5 GV decreases by about two orders of magnitude, to 0.03–0.24 cm^{-3} s^{-1}. Below about 7 km the profiles for R_c = 1 and 2 GV coincide, since only cascades of protons with rigidities above 2 GV reach these altitudes. The Monte Carlo statistical uncertainty is 1–5% around the ionization maximum. The calculations assume an isotropic proton flux and a sharp vertical cutoff and neglect the anisotropy of the event, the geomagnetic penumbra and the contribution of heavier nuclei. The results therefore represent an estimate of the ionization effect of GLE 77 at different geomagnetic latitudes.

Atmospheric ionization by solar cosmic rays via GEANT4

The figures below show the ionization profiles at 11:00 UT, when the solar proton spectrum is described by a power law with γ = 4.2. Compared with 10:20–10:30 UT, the change of the spectral shape affects the three cutoffs very differently. For R_c = 2 and 5 GV the profiles remain nearly unchanged: the maximum ionization rate is 75–680 cm^{-3} s^{-1} and 3.7–33 cm^{-3} s^{-1}, respectively, within about 15% of the values at 10:20–10:30 UT. In contrast, for R_c = 1 GV the ionization increases by a factor of about 8, reaching 1.3×10^3–1.1×10^4 cm^{-3} s^{-1}, and the maximum shifts upwards to about 19 km. This increase is caused by the steep rise of the power-law spectrum towards low energies, which strongly enhances the contribution of protons with rigidities between 1 and 2 GV (kinetic energies of 0.43–1.27 GeV). These protons are stopped mainly above the ionization maximum, and their effect is therefore most pronounced in the upper stratosphere and mesosphere. At 79 km the ionization rate for R_c = 1 GV is about 30 times higher than for R_c = 2 GV, compared with a factor of about 3 at 10:20–10:30 UT. As a result, at 11:00 UT the ionization effect of the event is concentrated at high geomagnetic latitudes, while at mid-latitudes it remains comparable to that in the initial phase. Since the lower boundary of the 1 GV integration (0.43 GeV) is close to the lower limit of the energy range in which the spectrum was derived (0.4 GeV), the results for R_c = 1 GV at this time are the most sensitive to the assumed spectral shape.


GLE #77, 11 November 2025
10:20-10:30 UT, proton; J0 min = 1e+05, J0 max = 9e+05
band: J0 min - J0 max
Rc = 1 GV
Rc = 2 GV
Rc = 5 GV
Altitude, km
Ionization rate, ion pairs cm⁻³ s⁻¹


GLE #77, 11 November 2025
11:00 UT, proton; J0 min = 1e+05, J0 max = 9e+05
band: J0 min - J0 max
Rc = 1 GV
Rc = 2 GV
Rc = 5 GV
Altitude, km
Ionization rate, ion pairs cm⁻³ s⁻¹

Conclusion

The atmospheric ionization caused by the solar protons of GLE 77 on 11 November 2025 was calculated with a GEANT4 Monte Carlo model of the atmosphere for four phases of the event and for geomagnetic cutoff rigidities of 1, 2 and 5 GV, corresponding to high, high-middle and middle geomagnetic latitudes. The main results can be summarized as follows.

1. In all phases of the event the ionization profiles have a maximum in the lower stratosphere, at 15–19 km, slightly above the Regener–Pfotzer maximum of the galactic cosmic ray ionization (13.5–14.5 km), owing to the softer spectrum of the solar protons.
2. The ionization effect depends strongly on the geomagnetic cutoff. At R_c = 1 GV the maximum ion pair production rate reaches 10^2–10^4 cm^{-3} s^{-1} and exceeds the galactic cosmic ray background many times. At R_c = 5 GV it is 3–33 cm^{-3} s^{-1} in the first hour of the event, comparable to the galactic cosmic ray ionization calculated for Sofia ([~17] cm^{-3} s^{-1}).
3. The temporal evolution of the spectrum controls the latitudinal distribution of the effect. The power-law spectrum at 11:00 UT produces the strongest ionization at high latitudes, while the progressive softening of the spectrum after 11:30 UT reduces the ionization at middle latitudes by about two orders of magnitude. In the late phase (15:00 UT) the direct ionization effect of the solar protons at middle latitudes is negligible compared with the galactic cosmic ray background, while at high latitudes it remains significant.
4. The cutoff dependence of the results follows closely the variation of the primary proton flux above the cutoff energy, which confirms that the spectral shape and its time evolution are the main factors determining the ionization effect of the event.

The results are subject to the uncertainty of the spectral normalization, which was taken into account as a range of J_0, and to the assumptions of an isotropic flux, a sharp cutoff rigidity and a purely proton composition. A more accurate estimate requires the time-resolved normalization of the spectrum, the anisotropy of the event and the contribution of helium and heavier nuclei. The developed computational framework can be applied to other GLE events and, combined with chemistry-climate models, used to assess the impact of intense solar particle events on the composition of the middle atmosphere.

References:

1. A.L. Mishev, B. Heber, K.L. Klein (2026). Ground level enhancement GLE #77 on 11 November 2025: a data summary. *Advances in Space Research*. https://doi.org/10.1016/j.asr.2026.03.023
2. Balabin, Yu. V., Gvozdevskiy, B. B., & Germanenko, A. V. (2026). GLE77 event of November 11, 2025. *Geomagnetism and Aeronomy*, 66(3), 499–514. https://doi.org/10.7868/S3034502226030038
3. Sato, T., et al. (2026). Estimation of global increase of radiation dose rates during the ground level enhancement on 11–12 November 2025 using WASAVIES. *Space Weather*. https://doi.org/10.1029/2026SW004949
4. Mishev, A. L., & Velinov, P. I. Y. (2018). Ion production and ionization effect in the atmosphere during the Bastille day GLE 59 due to high energy SEPs. *Advances in Space Research*, 61(1), 316–325. https://doi.org/10.1016/j.asr.2017.10.023
5. Pätsi, S., & Mishev, A. (2022). Ionization effect in the Earth's atmosphere due to cosmic rays during the GLE #71 on 17 May 2012. *Advances in Space Research*, 69(7), 2893–2901. https://doi.org/10.1016/j.asr.2022.02.008